Radiocarbon, Vol 60, Nr 1, 2018, p 91–112 DOI:10.1017/RDC.2017.62
© 2017 by the Arizona Board of Regents on behalf of the University of Arizona

DID SEA-LEVEL CHANGES AFFECT THE BRAZILIAN AMAZON FOREST DURING THE HOLOCENE?

Mayra Nina Araujo Silva[a] • Marcelo C L Cohen[a*] • Dilce F Rossetti[b] • Luiz C R Pessenda[c]

[a]Graduate Program of Geology and Geochemistry, Federal University of Pará. Av. Perimentral 2651, Terra Firme, 66077–530, Belém (PA), Brazil.
[b]National Space Research Institute (INPE), Rua dos Astronautas 1758–CP 515, CEP:12245–970, São José dos Campos (SP), Brazil.
[c]University of São Paulo, ^{14}C Laboratory, Av. Centenário 303, 13400–000, Piracicaba, São Paulo, Brazil.

ABSTRACT. In order to contribute to the discussion of Holocene climate changes, four sediment cores were collected from the northern Brazilian Amazonia lowland. These cores were studied through pollen analysis and sedimentary features, and the results were discussed within a chronological framework provided by radiocarbon dating. The cores were sampled from fluvial terraces representative of channel, floodplain/lake and crevasse splay deposits formed since the mid-Holocene. The pollen samples derive from floodplain/lake deposits and the pollen grains are mainly composed by families Moraceae, Euphorbiaceae, Caesalpiniaceae, Fabaceae, Rubiaceae, Melastomataceae, Combretaceae, Sapindaceae, Poaceae, Cyperaceae, Aizoaceae, Apiaceae and genus *Sebastiana*. The pollen data suggest no significant vegetation changes in the study area for the past 4808–4886 cal yr BP. This led to proposing stable climatic conditions since at least the middle Holocene. Such a finding is contrary to the occurrence of a dry period during the middle Holocene. The stabilization of the relative sea level about 6000 cal yr BP along the northern Brazilian littoral may have influenced the water table, and favored the establishment and maintenance of Amazonian lowland forest during the mid- and late Holocene. In addition, this process may have attenuated the impact of that dry period in areas under most fluvial influence.

KEYWORDS: Amazonia, Branco River, climate, Holocene, palynology, sea level.

INTRODUCTION

Several studies have indicated significant climatic changes in the Amazonian region during the Holocene. For instance, in lowland Amazonian Ecuador, periods of severe drought caused significant tree mortality between 8700 and 5800 cal yr BP, with more uniform conditions leading to the development of mature forests after 5800 cal yr BP (Weng et al. 2002). In the Colombian Amazonia, drier early Holocene and wetter late Holocene conditions were reported (Behling and Hooghiemstra 2000). Numerous authors have proposed that the dry Holocene period would have caused the replacement of forest by open savannah in several Amazonian areas, which was followed by forest during the late Holocene due to an increase of precipitation (e.g., Bush and Colinvaux 1988; Absy et al. 1991; Desjardins et al. 1996; Pessenda et al. 1998a, 1998b, 1998c, 2001; Behling and Hooghiemstra 1998, 1999, 2000; Freitas et al. 2001; Sifeddine et al. 1994 2001; Berrio et al. 2000; Weng et al. 2002; Behling 2011; Moreira et al. 2012; Hermanowki et al. 2012).

From 4000–3000 cal yr BP to the present, there was a moderate and progressive increase in arboreal vegetation in the southern Amazon basin, due to the return to more humid climate conditions that were probably similar to those of the the present day (Freitas et al. 2001; Pessenda et al. 2004). Isotopic studies in a southern Amazonian region and on a 1600-km transect covering three states of northeastern Amazonia indicated drier climate during the mid-Holocene and forest expansion associated with a wetter period during the last 3000 years (Pessenda et al. 1998a, 1998b, 1998c). Others studies have indicated that the climatic conditions in the Amazon Basin were drier during the early and mid-Holocene (e.g. Absy 1979; Gouveia et al. 1997; Behling and Costa 2000; Sifeddine et al. 1994; Mayle et al. 2000; Sifeddine et al. 2001; Cordeiro et al. 2008; Mayle and Power 2008; Hermanowski et al. 2012) and changed to a wetter climate during the late Holocene (e.g. Behling and Costa 2000; Bush et al. 2007; Cordeiro et al. 2008).

*Corresponding author. Email: mcohen80@hotmail.com.

https://doi.org/10.1017/RDC.2017.62 Published online by Cambridge University Press

There is still a lack of consensus about the Holocene climate, and particularly about the presence of a middle Holocene dry period in the Brazilian Amazonian lowland. For instance, several authors have defended that there is no evidence for a significant climatic change during most of the Holocene (e.g., Behling and Costa 2000; Bush et al. 2000; Behling et al. 2001; Irion et al. 2006; Miranda et al. 2009; Castro et al. 2010; Zani et al. 2012). This debate motivated us present this work, which provides pollen and radiocarbon (^{14}C) data of deposits from old fluvial terraces along the Branco River in northeastern Amazonia. These data allow to reconstruct vegetation patterns for the past 5000 cal yr BP and further discuss about the climate that prevailed in this area during this time frame.

STUDY AREA

The study area is located along the Branco River in the State of Roraima (Figure 1). The Branco River basin is formed by the junction of the Tacutu and Urariocoera Rivers, about 30 km upstream of the city of Boa Vista. The segment of the Branco River studied here is located approximately 550 km northward of its confluence with the Negro River (Figure 1). This area is inserted in the Pantanal Setentrional Basin, an area of Quaternary sediments (Santos et al. 1993) mainly formed in megafan depositional systems (Rossetti et al. 2014), which is bounded to the north, east, and west by Precambrian crystalline rocks of the Guiana Shield. The study area encompasses late Pleistocene to Holocene sands and muds surrounded by alluvial deposits of the Plio-Pleistocene Içá Formation (RADAMBRASIL 1976).

A typical tropical climate, with a well-defined dry season and an average annual rainfall between 1700 and 2000 mm/year prevails in the study area. Average annual temperatures range from 26°C to 33°C (RADAMBRASIL 1975). The Intertropical Convergence Zone (ITCZ) and the El Niño/La Niña–Southern Oscillation (ENSO) play important roles on the interannual rainfall regime in this region (Latrubesse and Nelson 2001).

The State of Roraima has a vegetation cover represented by a mosaic that consists of large areas of open vegetation either intermingled or in sharp contact with the Amazonian rainforest (Serruya 2002; Ab'Saber 1989). The latter show variation in physiognomy and structure according to their environment. The forest vary from *várzea*, *igapó*, and hilltop "islands" with *terra-firme* forest (Gribel 2009; Laranjeiras et al. 2014). Fluvial plains are dominated by *várzea* forest mainly represented by Arecaceae (Veloso et al. 1991). In these lowland areas, trees are relatively thick, with heights between 30 and 40 m near drainages. This vegetation is mainly represented by Annonaceae, Burseraceae, Humiriaceae, Euphorbiaceae, Myrtaceae, Melastomataceae, Apocynaceae, and Vochysiaceae, among others (IBGE 2012). In addition, the study area also contains white-sand forest locally known as *campina* or *campinarana*, with various types (i.e., grassland, shrubland, arboreous, or forest campinaranas; Gribel 2009) However, *campinaranas* are more generally characterized by Poaceae and Cyperaceae, which are surrounded by the rainforest mainly represented by Bombacaceae, Euphorbiaceae, Sapotaceae, Moraceae, Fabaceae, Malpighiaceae, Rubiaceae, Bignoniaceae, Rubiaceae, Melastomataceae, Arecaceae, *Mouriri sp*., *Sacoglottis guianensis*, and *Caraipa savannarrum* (Anderson 1981; Gribel et al. 2009).

MATERIAL AND METHODS

Field Sampling and Sediment Description

In order to obtain a continuous pollen record throughout the Holocene, 10 cores were sampled depths up to 10 m using a Russian sampler. However, only four cores presented suitable pollen

https://doi.org/10.1017/RDC.2017.62 Published online by Cambridge University Press

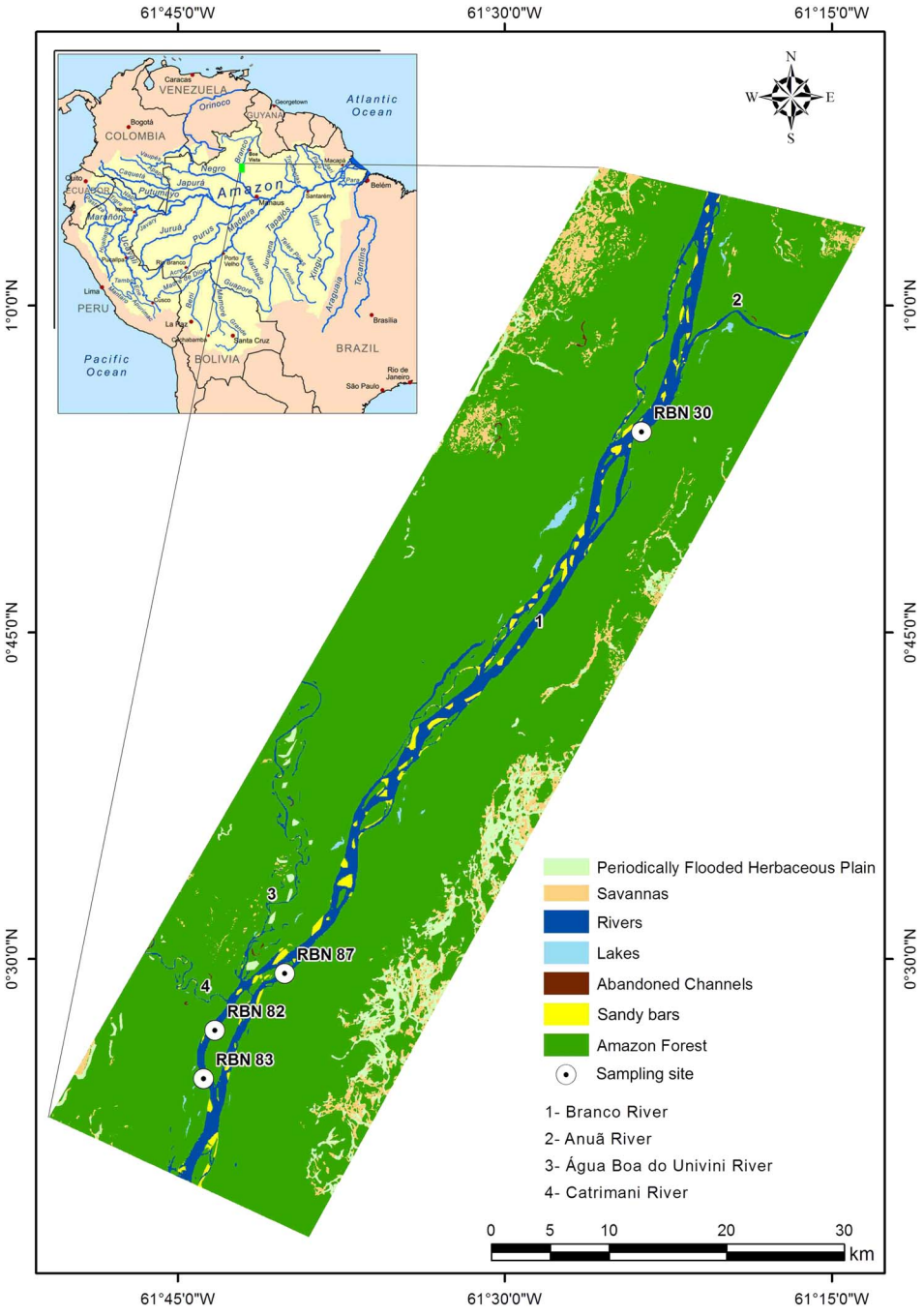


Figure 1 Location of the study area showing the geomorphological features and vegetation units along the Branco River.

concentration to a consistent statistical analysis. Three cores were taken from old fluvial terraces located about 10 m higher than the modern floodplain at the margin of the Branco River (Figure 1), and they were named RBN 30 (0°54′11.9′′N, 61°23′41.8′′W), RBN 82 (0°26′42.7′′N,

https://doi.org/10.1017/RDC.2017.62 Published online by Cambridge University Press

61°43′16.1′′W), and RBN 83 (0°24′29.4′′N, 61°43′47.0′′W). One core, RBN 87 (0°29′19.9′′N, 61°40′04.3′′W) was sampled from an abandoned channel (Figure 1). These sampling sites are dominated by dense rainforest.

Facies descriptions included observations of lithology, texture and structure, and they aimed interpretation of depositional environments. These sedimentary characteristics were recorded on a measured lithostratigraphic profile. Grain size for the interval with pollen data was determined in more detail by laser diffraction using a Laser Particle Size SHIMADZU SALD 2101 in the Laboratory of Chemical Oceanography/UFPA. Prior to grain size analysis, approximately 0.5 g of each sample was immersed in H_2O_2 to remove organic matter, and the residual sediments were disaggregated by ultrasound (França et al. 2012). The grain-size scale of Wentworth (1922) was used in this work with sand (2–0.0625 μm), silt (62.5–3.9 μm), and clay fractions (3.9–0.12 μm).

Pollen Analysis

For pollen analysis, 1.0 cm^3 of sediment were collected in intervals of 2.5 (RBN 30) and 5 cm (RBN 82, 83, and 87), which totaled 85 samples. All samples were prepared using standard pollen analytical techniques including acetolysis (Faegri and Iversen 1989). Sample residues were mounted on slides in glycerin jelly. Pollen and spores were identified by comparison with reference collections of about 4000 Brazilian forest taxa and various pollen keys (Salgado-Labouriau 1973; Absy 1975; Markgraf and D'Antoni 1978; Roubik and Moreno 1991; Colinvaux et al. 1999), jointly with the reference collections of the Laboratory of Coastal Dynamics–Federal University of Pará and ^{14}C Laboratory of the Center for Nuclear Energy in Agriculture (CENA/USP) to identify pollen grains and spores. A minimum of 300 pollen grains were usually counted for each sample, but for some specific depths 200 or 250 grains were counted due to their low pollen concentrations. Microfossils consisting of spores, algae, and some fungi were also counted, but they were not included in the sum.

All pollen taxa present were identified, but only the most abundant were plotted in pollen diagrams in order to illustrate the different ecological groups. The pollen diagrams were statistically subdivided into assemblage zones using a square-root transformation of the percentage data, followed by stratigraphically constrained cluster analysis (Grimm 1987). The intervals not analyzed by pollen content along the stratigraphic profiles exhibit absolute absence of pollen.

Radiocarbon Dating

Based on lithostratigraphic changes, seven samples of sedimentary organic matter (10 g each) were selected for ^{14}C analysis, two in each of the cores Rbn82, Rbn83, Rbn30, and one in core Rbn87. Dating was carried out at the BETA Analytic Laboratory and LACUFF (Fluminense Federal University–Brazil) using accelerator mass spectrometers (AMS).

At the BETA Analytic Laboratory, sample pretreatment and dating followed the Beta Analytic for Radiocarbon Dating Laboratory standard technique for accelerator mass spectrometry (AMS) dating. The pretreatment consisted of dispersing the sediment deionized water, followed by sieving through 180-micron sieve to recover any available plant material and to remove any stones, gravel or other course inorganic grains. The less than 180-micron size fraction was used in each case. Two 0.1N HCl baths where applied for 2 hr each at 70ºC to remove any carbonates. Samples were rinsed to neutral and dried at 100ºC for 12 hr, cooled and weighed. After homogenizing with mortar and pestle, a small portion of the sediment was tested under a

https://doi.org/10.1017/RDC.2017.62 Published online by Cambridge University Press

microscope with 12M HCl to ensure complete removal of all carbonate. Each sample was subsampled and combusted to CO_2 in a closed chemistry line which has been purged of any CO_2 to a level below 10e–15 atoms (background levels). The CO_2 was then introduced into a reaction vessel containing an aliquot of cobalt metal catalyst. Hydrogen was introduced such that when the cocktail was heated to 500ºC, the CO_2 cracked to carbon (graphite). The graphite was pressed into a target for measurement in an AMS system. The AMS was calibrated to provide an accurate ratio of the $^{14}C/^{13}C$ ratio between the sample graphite and a modern reference (NIST–4990C, oxalic acid). Quality assurance (QA) samples were reacted simultaneously in the chemistry lab and measured simultaneously in the AMS. The analytical result was obtained as a fraction of the value of modern reference, corrected for isotopic fractionation using $^{13}C/^{12}C$ ($\delta^{13}C$) and ^{14}C age calculated according to the conventions cited in Stuiver and Polach (1977). The QA samples were checked for accuracy and observed to fall within expectations for the laboratory to accept and report the sample results. The QA acceptance was defined as the total laboratory error known to be within 2σ. The equipment used in these analyses were the Thermo Delta-Plus isotope ratio mass spectrometer ($\delta^{13}C$ precision of ± 0.3‰) and the 250 kV NEC single stage particle accelerator (AMS precision of ± 0.001 – 0.004 fractions modern) (http://www.radiocarbon.com/PDF/Beta-AMS-Methodology.pdf).

The samples dated at the LACUFF were previously examined and physically cleaned under a stereomicroscope. The organic matter (humin) from sediment samples were extracted according to the laboratory standard pretreatment with the acid–alkali–acid method (Pessenda et. al. 1996). At LACUFF, the samples were converted to carbon dioxide organic samples and all gas samples were cryogenically purified. Graphitization method and other procedures in the LACUFF laboratory can be obtained in Macario et al. (2013). Results are expressed as radiocarbon ages (^{14}C yr BP) normalized to a $\delta^{13}C$ of –25‰ PDB, presently denoted as VPDB, or percentage of modern carbon (pMC) (Stuiver and Polach 1977). ^{14}C ages were also reported as calibrated years [cal yr BP, 2σ using CALIB 7.1 software and SHcal13 curve (Reimer 2013) and CALIBomb (Reimer et al. 2004)].

RESULTS

^{14}C and Sedimentation Rates

The validity of ^{14}C dates extracted from organic matter in sedimentary environments such as lakes, bogs, and fluvial plains has been evaluated (Turney et al. 2000; Lowe et al. 2004; Howard et al. 2009), and extensively used to provide robust chronologies for landscape evolution, particularly the timing and correlation of climatic and sea-level-change events (e.g. Pessenda et al. 2012; Cohen et al. 2014, 2012; Rossetti et al. 2015). Howard et al. (2009) tested the validity of ^{14}C dating in fluvial sedimentary deposits and the humin and humic acid fraction dating revealed results statistically consistent, where the humin and humic acid fraction provide the more reliable age estimates for each dated sample depth in fluvial sediments. In addition, this study revealed that plant macrofossils produce younger dates than the humic and humin fractions. Regarding our ^{14}C dates, obtained along cores sampled from fluvial plains, these data provide a coherent chronological framework for a lithostratigraphic and pollen analysis (Table 1). No age reversal was recorded. The oldest ages were recorded at the base of the lithostratigraphic profile from where core RBN 83 was acquired. The age of 4808–4886 cal yr BP was obtained from the middle part of this core, and another age of 4223–4414 cal yr BP occurs in the first overlying mud, located only 0.6 m upward. Core RBN 82 was acquired at the top of a lithostratigraphic profile displaying ages of 1576–1718 and 1319–1486 cal yr BP. The pollen profile RBN 30 was dated at the base at 1303–1482 yr BP and at the top as 310–486 cal yr BP.

https://doi.org/10.1017/RDC.2017.62 Published online by Cambridge University Press

Table 1 Sediment samples selected for radiocarbon dating with material depth ^{14}C conventional and calibrated ages (using Calib 7.1 and SHcal13 curve, Reimer et al. 2013; and CALIBomb, Reimer et al. 2004).

Cody site and laboratory number	Core	Depth (cm)	Material	Ages (^{14}C yr BP 1σ)	Ages (cal yr BP 2σ deviation)
BETA353352	Rbn83	490	Bulk sed.	4310 ± 30	4808–4886
BETA353350	Rbn83	430	Bulk sed.	3910 ± 30	4223–4414
BETA353346	Rbn82	850	Bulk sed.	1780 ± 30	1576–1718
BETA353348	Rbn82	350	Bulk sed.	1560 ± 30	1319–1486
LACUFF140158	Rbn30	190	Bulk sed.	1534 ± 41	1303–1482
LACUFF140159	Rbn30	165	Bulk sed.	366 ± 41	310–486
BETA353356	Rbn87	240	Bulk sed.	110.3 ± 0.4 pMC	1957*

*Cal AD.

The youngest age was recorded at the base of pollen profile RBN87, revealing a modern ^{14}C content indicative of post-thermonuclear testing era (110.3% ± 0.4 pMC 1957 cal AD), indicating an essentially modern age.

Considering a linear interpolation between age control points, the sedimentation rate in core RBN 82 is 20 mm/yr (850–350 cm). RBN 83 presents rates between 1.13 (490–430 cm) and 0.98 mm/yr (430–0 cm), and RBN 30 core presents rates about 0.25 mm/yr (190–165 cm) and RBN 87 presents 43 mm/yr (240–0 cm). As noted in some studies in the northern Amazon (Behling et al. 2004; Cohen et al. 2005a, 2008, 2009; Vedel et al. 2006; Guimarães et al. 2010) these differences in sedimentation rates are related to the settling velocity of sediments, since larger diameter particles (e.g. gravel and sand) settle faster than fine particles (e.g. silt and mud), and water velocities necessary to carry large particles in suspension are greater than those needed to keep fine particles suspended.

Sediment Description

Core RBN 87 was acquired from a succession of circa 3-m-thick sediments, represented muddy deposits interbedded by sands (Figure 2). The latter display sharp, erosional, and concave-up bases, and they grade upward from coarse/medium- to medium/fine- and then fine-grained. These deposits are massive, moderate to well sorted, and mostly composed by quartz grains. The muddy sediments are either massive or parallel-laminated and they vary from light to dark gray in color. Core RBN 87 was obtained between 2.4 and 2 m depth, and consists only of dark gray, parallel-laminated muds with abundant plant remains. Detailed grain size analysis revealed a composition of 45% clay, 50% silt, and 5% sand. These deposits occur in a concave-up morphology, grading downward into massive sands to complete a fining upward succession. Upward, they are sharply overlain by a thicker, i.e., up to 2-m-thick fining upward sandy succession.

RBN 83 was acquired from a 5.2-m-thick river bank composed of sands and muds distributed in almost equivalent proportion (Figure 3). The sandy deposits have grain sizes similar to RBN87, they also fine upward, and are based by sharp and erosional and concave-up surfaces. Most of the muds occur outside the concave-up shapes, and they display light gray to greenish colors. Core RBN83 records the lowermost 0.7 cm of this lithostratigraphic profile, being represented by at the base by 0.3 cm thick massive greenish gray mud and 40-cm-thick peat layer at the top. Interesting is that, despite the muddy nature, the contact between these deposits is defined by a sharp and also slightly concave-up discontinuity surface. Detailed grain-size analysis revealed mean values for clay of 25%, silt of 60%, and sand of 15%.

https://doi.org/10.1017/RDC.2017.62 Published online by Cambridge University Press

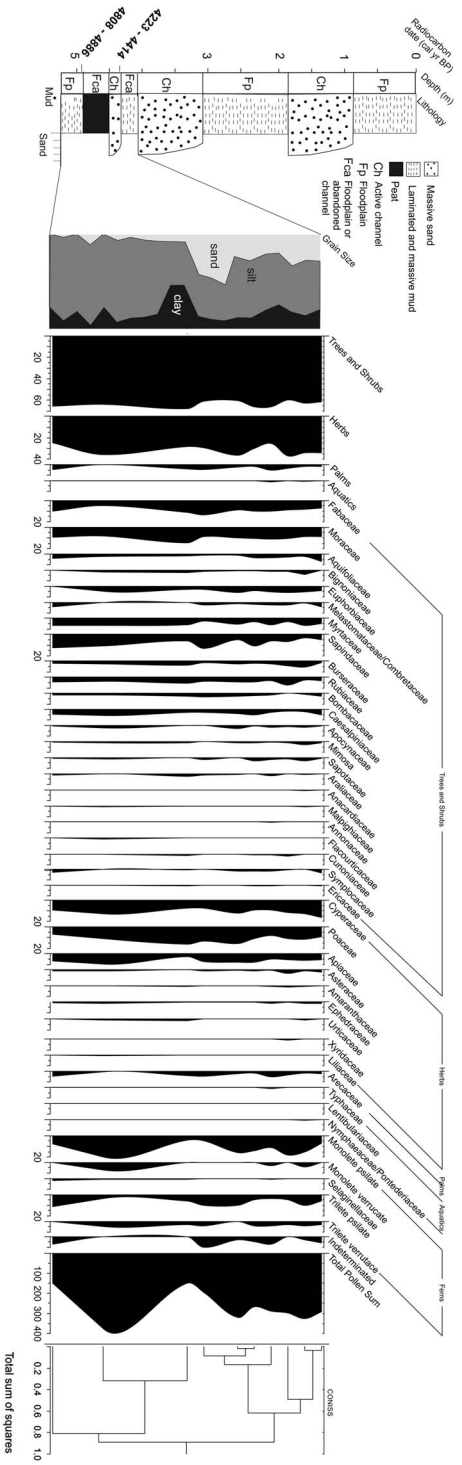


Figure 2 Summarized results for core Rbn-83 with variation as a function of core depth showing chronological and lithological profiles with sedimentary facies as well as ecological pollen groups and percentages of the most frequent pollen taxa zones and cluster analysis.

https://doi.org/10.1017/RDC.2017.62 Published online by Cambridge University Press

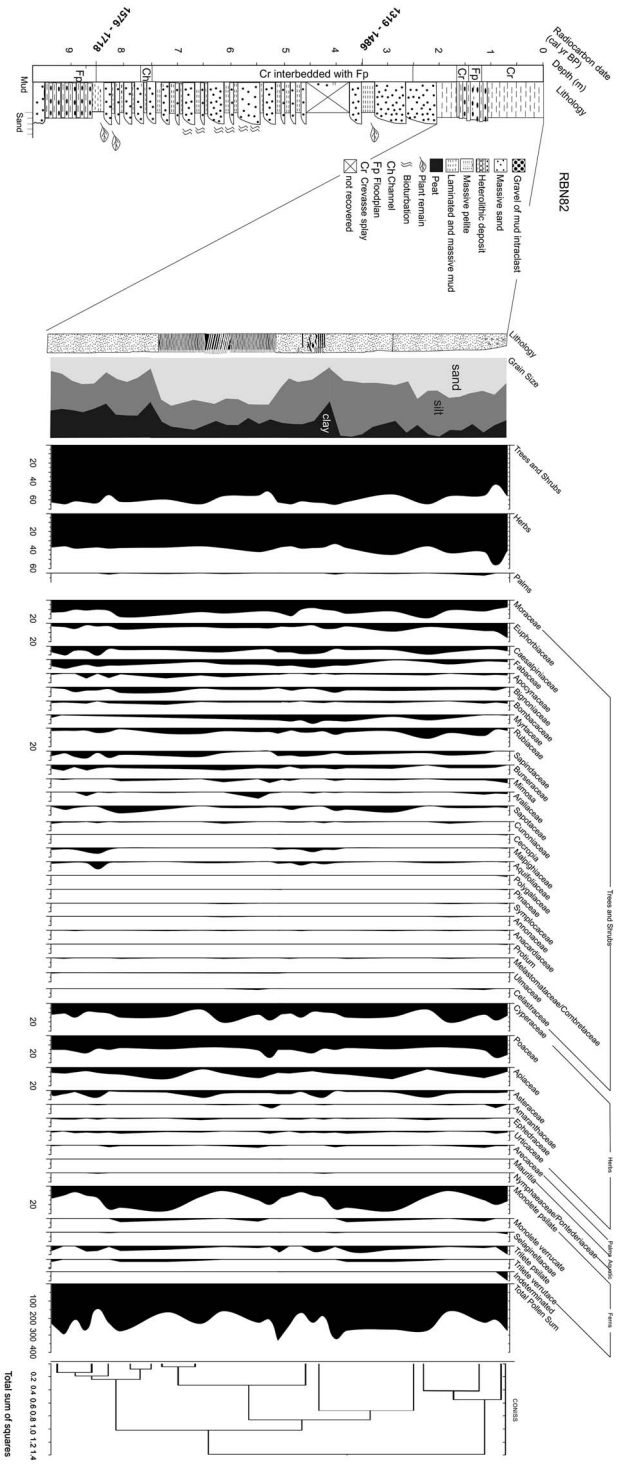


Figure 3 Summarized results for core Rbn-82 with variation as a function of core depth showing chronological and lithological profiles with sedimentary facies as well as ecological pollen groups and percentages of the most frequent pollen taxa zones and cluster analysis.

https://doi.org/10.1017/RDC.2017.62 Published online by Cambridge University Press

RBN 82 derives from a 9.7-m-thick sedimentary succession (Figure 4) also consisting of interbedded sands and muds, but which displays a vertical organization completely different from the two previously described profiles. Hence, sand beds are progressively thicker upward, configuring an overall thickening upward succession. In addition, individual sand beds, which are massive or bioturbated and lenticular in shape, grade upward from very fine to fine-, or fine to medium-grained. Downward, they grade into mud layers, completing several coarsening upward successions. As opposed to their gradational basis, the top of the sand beds is essentially sharp. The muds in this profile vary from light to dark gray. They are massive or parallel-laminated and locally they alternate rhythmically with sand laminae to form lenticular heterolithic bedddings. Core RBN82 was acquired at the topo of this succession, where a 2.2-m-thick interval of dark gray organic mud is present. Detailed grain-size analysis revealed mean values of 20% clay 20%, 40% silt, and 40% sand.

RBN 30 derives from a 4.5-m-thick sedimentary succession consisting of muds and sands arranged into fining upward cycles (Figure 5). Three of these cycles are present, which were caused by sharp and erosional discontinuity surfaces mantled by coarse-grained sands or gravel with mud intraclasts. Upward, these deposits grade into medium- and then fine-grained sands, or they grade directly into laminated or massive muds, as well as massive pelite. RBN30 was acquired from a 0.6-cm-thick interval consisting of dark-gray, organic muds with parallel lamination that overlie directly a package of gravel with mud intraclast. Detailed grain-size analysis revealed mean values of 40% clay, 55% silt, and 5% sand.

Pollen Analysis

Seventy pollen taxa were identified (Table 2), but the diagrams (Figures 2–5) show only the most abundant taxa (>3% pollen sum) and the different ecological groups. The pollen grains identified in the core RBN83 was accumulated between 4808–4886 and 4223–4414 cal yr BP. Trees and shrubs pollen dominate the pollen assemblage (60–68%), and they are mainly represented by Sapindaceae (7–16%), Fabaceae (5–15%), Moraceae (10–15%), Myrtaceae (5–8%), Rubiaceae (5–8%), Aquifoliaceae (0–7%), Bignoniaceae (0–5%), Euphorbiaceae (1–5%), Melastomataceae/Combretaceae (0–5%), Bombacaceae (0–3%) and Sapotaceae (0–4%), while herb pollen (25–38%) are mainly characterized by Cyperaceae (7–18%), Poaceae (10–17%) and Apiaceae (5–10%) and Asteraceae (0–3%). Arecaceae presents low percentages (0–3%).

The pollen content of the RBN30, deposited between 1303–1482 and 310–486 cal yr BP, presents trees and shrubs (45–78%) mainly consisting of *Sebastiana* (0–43%), Fabaceae (5–25%), Melastomataceae/Combretaceae (5–15%), Euphobiaceae (2–15%), Sapotaceae (0–9%), Rubiaceae (2–15%), Moraceae (0–5%), Apocynaceae (0–6%), *Byrsonima* (0–10%), Myrtaceae (0–8%), *Didymopanax* (0–3%), Malpighiacaeae (0–5%). Herb pollen (25–48%) are mostly characterized by Poaceae (16–45%), Aizoaceae (2–10%), Solanaceae (0–10%), and Cyperaceae (0–3%).

Considering the mean sedimentation rates obtained to RBN82, the pollen assemblage analysed was accumulated during the last 1576–1718 cal yr BP. Trees and shrubs (45–65%) dominate the pollen profile, which is mainly represented by Moraceae (8–25%), Euphorbiaceae (3–15%), Caesalpiniaceae (5–10%), Fabaceae (2–10%) Rubiaceae (1–11%), Apocynaceae (0–5%), Bignoniaceae (1–6%), Bombacaceae (0–4%), Sapotaceae (0–9%), Myrtaceae (0–10%), Sapindaceae (0–8%), Burseraceae (0–5%), Araliaceae (0–6%), and Malpighiaceae (0–6%). Herb pollen

https://doi.org/10.1017/RDC.2017.62 Published online by Cambridge University Press

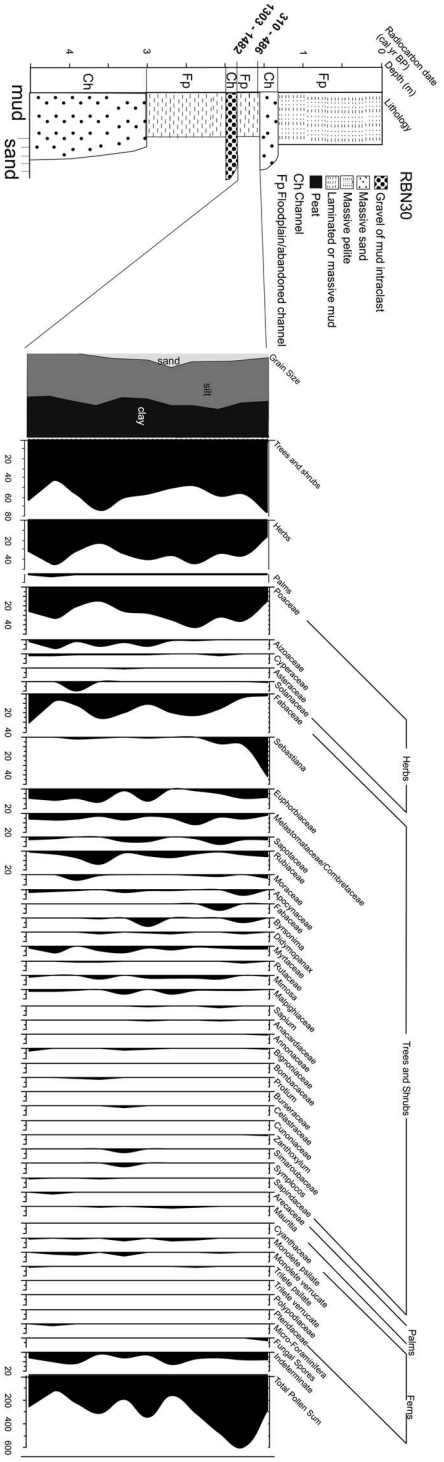


Figure 4 Summarized results for core Rbn-30 with variation as a function of core depth showing chronological and lithological profiles with sedimentary facies as well as ecological pollen groups and percentages of the most frequent pollen taxa.

https://doi.org/10.1017/RDC.2017.62 Published online by Cambridge University Press

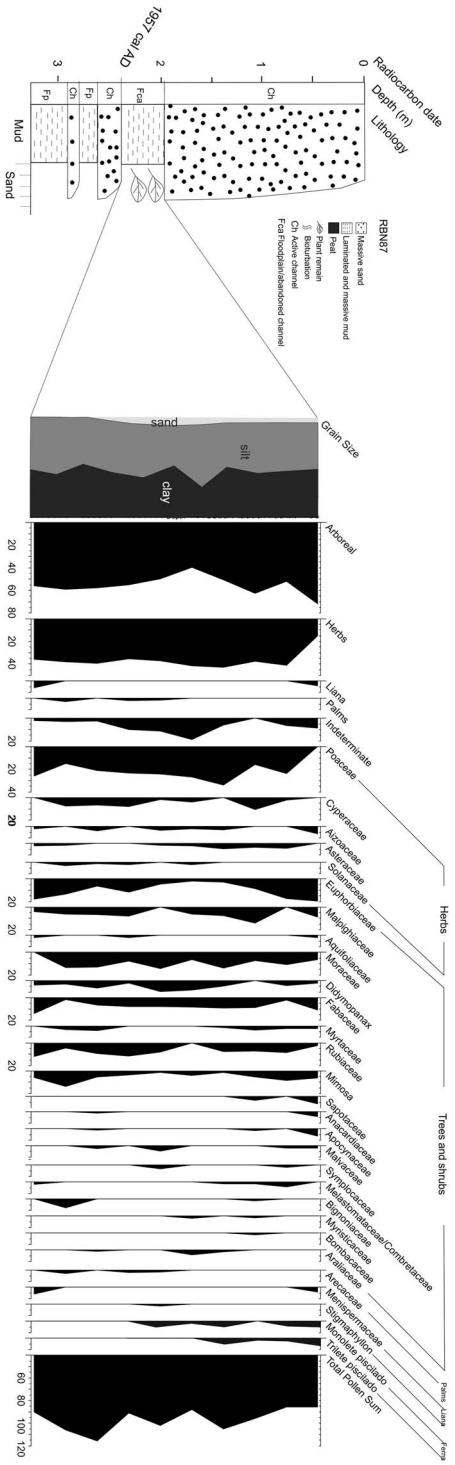


Figure 5 Summarized results for core Rbn-87 with variation as a function of core depth showing chronological and lithological profiles with sedimentary facies as well as ecological pollen groups and percentages of the most frequent pollen taxa.

https://doi.org/10.1017/RDC.2017.62 Published online by Cambridge University Press

Table 2 Taxa identified in the studied cores.

Family *Genus*	Family *Genus*
Acanthaceae	Malpighiaceae
Aizoaceae	Malpighiaceae
Amaranthaceae	*Byrsonima*
Amaranthaceae/Chenopodiaceae	Malvaceae
Anacardiaceae	Malvaceae
Annonaceae	Melastomataceae/Combretaceae
Apiaceae	Menispermaceae
Apocynaceae	Mimosaceae
Aquifoliaceae	*Mimosa*
Araliaceae	Moraceae
Didymopanax	Myristicaceae
Arecaceae	Myrsinaceae
Mauritia	Myrtaceae
Asteraceae	Nymphaeaceae/Pontederiaceae
Bignoniaceae	Poaceae
Bombacaceae	Polygalaceae
Burseraceae	Proteaceae
Protium	Rubiaceae
Caesalpiniaceae	*Coccocypselum*
Celastraceae	*Psychotria*
Chloranthaceae	Rutaceae
Cunoniaceae	*Zanthoxylum*
Cunoniaceae	Sapindaceae
Cyanthaceae	Sapotaceae
Cyperaceae	Selaginelaceae
Ephendraceae	Simaroubaceae
Ericaceae	Solanaceae
Euphorbiaceae	Symplocaceae
Sapium	*Symplocos*
Sebastiana	Typhaceae
Fabaceae	Ulmaceae
Flacourticaceae	Urticaceae
Hyppocrateaceae	*Cecropia*
Lentibulariaceae	Verbenaceae
Liliaceae	Xyridaceae

(35–55%) are mainly evidenced by Poaceae (15–25%), Cyperaceae (10–20%), Apiaceae (2–12%), Asteraceae (1–7%), and Amaranthaceae (0–4%).

The pollen assemblage obtained from core RBN87 was deposited after 1957 cal AD. This pollen profile is dominated by the high abundance of trees and shrubs (40–73%), which are mainly characterized by Euphorbiaceae (2–20%), Moraceae (7–15%), Fabaceae (3–15%), Malpighiaceae (2–15%), *Didymopanax* (0–10%), Myrtaceae (0–5%), Rubiaceae (0–12%), Sapotaceae (0–6%), Bignoniaceae (0–7%), and Melastomataceae/Combretaceae (0–5%). Herb pollen (16–44%) are mostly represented by Poaceae (2–35%), Mimosa (2–14%), Cyperaceae (2–11%), Aizoaceae (0–7%), and Asteraceae (0–5%).

https://doi.org/10.1017/RDC.2017.62 Published online by Cambridge University Press

INTERPRETATION AND DISCUSSION

The lithostratigraphic profiles containing the pollen cores described in this study are dominated by sequences of sandy sediments grading upward into mud deposits. These vertical changes, with grain-size decreases with height above the base, characterize fining upward cycles. This structure is consistent with stratigraphic successions developed according to the local fluvial dynamics. Fluvial deposits commonly consist of fining-upward facies successions (Walker 1992). The sharp, erosional, and concave-up bases of individual sandy packages conform with deposition in confined environments, typical of channels. Mud deposits overlying these channels were either formed by mud settling from suspensions in abandoned channels or nearby floodplains. Muds formed overlying concave up sharp discontinuity surfaces, as recorded in RBN83, are probably the record of stagnant conditions within mud plugs or small lakes developed along floodplains.

On the other hand, the several coarsening upward lenses recorded in the lithostratigraphic profile, where core RBN 82 was acquired, records a distinct sedimentary process. In this instance, the upward increase in grain size indicates increasing flow energy through time. Considering deposition in a fluvial system, the occurrence of sandy lenses having this characteristic gradationally overlying muds is more likely attributed to episodic sand inflow within low energy environments dominated by mud deposition from suspensions. Such a situation is commonly verified during flooding, when fluvial channels cannot bear their flows, and discharge into adjacent floodplains, forming crevasse splays. Hence, this lithostratigraphic profile records a succession of crevasse splay deposits formed during progressively increased flooding, with the top muds recorded by the core RBN 82 representing the return to normal conditions, when the floodplain was again dominated by low energy mud settling.

The modern hydrographic basin of the Branco River presents many abandoned channels and oxbow lakes along its floodplain (Figure 1). These geomorphologic features are caused by channel shifting, which results in meander cutoff and channel-belt avulsion (Toonen et al. 2012). They are identified in the study site as depressions of considerable reduced width and depth. These features result from autogenic processes inherent to sedimentary dynamics. They represent depressions that are sediment traps with high preservation potential to pollen grains (Kasse et al. 2005; Bos et al. 2008; Cohen et al. 2014), as indicated by the analysis of the studied fluvial deposits preserved along the Branco River terraces.

Lakes and floodplains generally provide suitable conditions for mud accumulation and preservation of pollen grains sourced by vegetation from the time that sediment was deposited. Lacustrine sediments preserve pollen sourced from vegetation surrounding the lakes, and the spatial representativeness of the lacustrine pollen signal depends on the winds and the extension of the drainage system. The proportion of the pollen signal provided by each vegetation type is distance-weighted (e.g. Davis 2000; Xu et al. 2012). Open vegetation is likely to have a higher proportion of long-distance transport pollen rain, but under a relatively closed canopy the sediment should record a small spatial representation of the nearby vegetation (Weng et al. 2004b; Gosling et al. 2009). Our stratigraphic record during the middle and late Holocene showed predominantly arboreal vegetation, whose pollen were probably accumulated around relatively small body of water of floodplain areas similar to those found today in the study site (Figure 1). Such a condition may have attenuated the eventual effect of wind transport. Thus, the pollen profile should represent the paleovegetation of this drainage basin.

Therefore, the analyzed sediments, accumulated during the middle and late Holocene, indicate a mixture of forest vegetation and herbaceous communities comparable to the local modern vegetation (Figure 6). Considering a dry climatic phase until the middle Holocene, it would cause

https://doi.org/10.1017/RDC.2017.62 Published online by Cambridge University Press

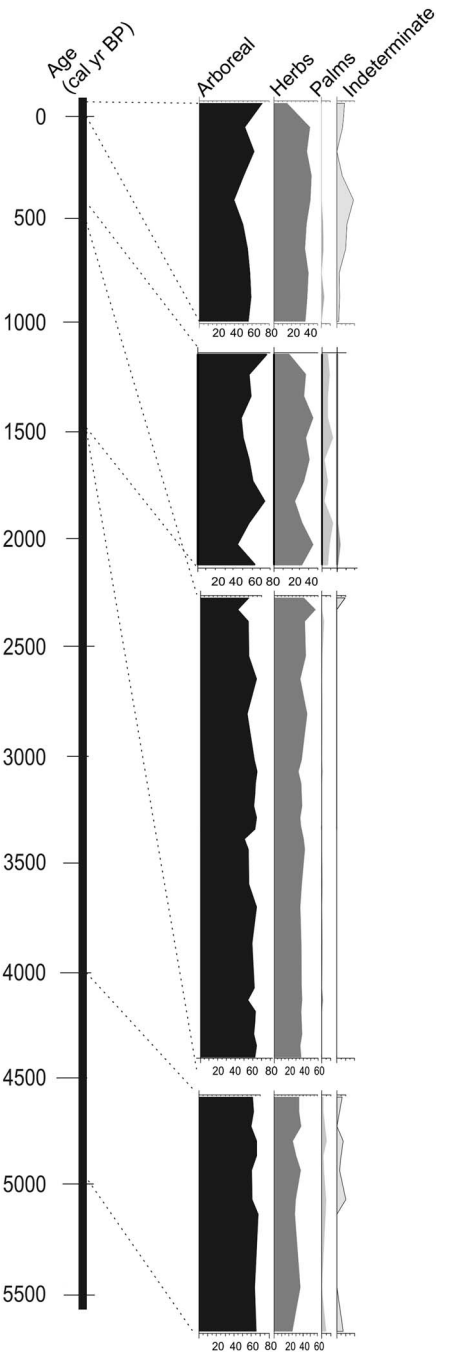


Figure 6 Temporal integration of the ecological pollen groups identified in studied cores.

an expansion of herbaceous in detriment of arboreal vegetation in the study area, producing a significant increase in percentage of herbs pollen grains along the sediments accumulated during the middle Holocene. Such evidence has not been recorded in the core Rbn83 (Figure 2).

https://doi.org/10.1017/RDC.2017.62 Published online by Cambridge University Press

Causes for Vegetation Stability During the Middle and Late Holocene

The modern plant distribution in the Amazonian region has been widely debated, with main hypotheses having considered the influence of climate (ter Steege et al. 2003; Ruter et al. 2004), topography (Vormisto et al. 2000), soil (ter Steege et al. 1993), and geology (Räsänen et al. 1987; Van der Hammen et al. 1992; Zani et al. 2012). In this context, patches of open vegetation that are commonly found intermingled with the Amazonian rainforest have been interpreted as remnants of a vegetation cover formed due to the presence of a dry period during the late Pleistocene (Ledru et al. 2006) and early to middle Holocene (Freitas et al. 2001; Pessenda et al. 2001, 2004).

Some works propose changes in the physical environment as the main factor to the establishment of vegetation patterns in Amazonia through time, as well as other areas around the globe (Van der Hammen et al. 1992; Behling and Hooghiemstra 2000; Maslin and Burns 2000; Freitas et al. 2001; Sifeddine et al. 2001; Mayle and Power 2008). For instance, the climate changed gradually from dry to wetter after the Last Glacial Maximum (LGM), which appears to have been accompanied by changes in the fluvial discharge (Latrubesse and Ramonell 1994; Latrubesse 2002; Rigsby et al. 2009). An increment of up to 40% of humidity after the Younger Dryas was proposed for this region (Maslin and Burns 2000).

The prevalence of wet conditions since the middle Holocene has been proposed for several areas of the Brazilian Amazonia (Maslin and Burns 2000; Pessenda et al. 2001; Sifeddine et al. 2001; Rossetti et al. 2004, 2005; Jacob et al. 2007; Cordeiro et al. 2011), which coincided with the expansion of tropical forest as we know it today. The melting of the global ice volume during the transition from the last glacial stage into the current interglacial phase culminated with the global rise in sea level of up to 5 m above the modern sea level in the middle Holocene (Shackleton 1988), which consequently caused an increase of humidity. Climatic and sea-level changes during the Holocene influenced significantly the development of mangrove along coastal Amazonian areas (e.g., Cohen et al. 2012).

The data presented here indicate a mixture of forest and herbaceous communities comparable to the modern vegetation mosaic of the study area (Figure 6). They also suggest a wet period at least over the last 4808–4886 cal yr BP, without any indication of an expressive vegetation change as a consequence of any eventual middle Holocene dry event.

Some hypotheses may be raised to justify the stability of vegetation patterns in the study site since the middle Holocene. Hence, one possibility is that many Amazonian areas were not under the effect of dry climates during this time frame. In fact, speleothem oxygen isotope indicates that ecosystems in western Amazonia have not experienced prolonged drying over the past 94,000 years (Mosblech et al. 2012). In addition, an integrated approach combining pollen and diatom data from the Marajó Island, located at the mouth of the Amazon River in northeastern Amazonia, recorded no significant change in vegetation during the late Pleistocene through the early/mid Holocene (Castro et al. 2013). A drastic middle Holocene change from forest to grassland vegetation was related by these authors to sedimentary influence resulting from coast progradation due to a drop in relative sea-level rather than a drier climate, because these are dominantly C_3 herbs typical of wet areas (see also Miranda et al. 2009 and Castro et al. 2010). C and N isotope analyses of organic matter from sediments from an area of northern Amazonia located only around 30 km to the east of the study area (Zani et al. 2012) led to state asyncronical development of open vegetation during the middle to late Holocene which was controlled by sedimentary dynamics, rather than climatic changes. In addition, no evidence of mid-Holocene dry climate was found in lakes near Prainha, central Amazonia (Bush et al. 2000). Furthermore, a continuous record of

https://doi.org/10.1017/RDC.2017.62 Published online by Cambridge University Press

forests was documented in the Caxiuaná area, northeastern Amazonia, for the last 7800–7940 cal yr BP (Behling and Costa 2000). Lake Calado, near Manaus, displayed dense tropical forest since 8280–8380 cal yr BP (Behling et al. 2001). Several works stated that the Amazonia rainforest was most likely undisturbed during the last 50,000 years (e.g., Colinvaux et al. 1996, 2001; Bush et al. 2004; Irion et al. 2006; Toledo and Bush 2007; Mayle and Power 2008).

Another possibility to consider is that the impact of the dry period, claimed by several authors to have occurred in this region during the early and middle Holocene, did not influence this particular site of the Amazonian forest. It is interestingly to mention that, in contrast to many other Amazonian areas, this particular region currently displays a peculiar climatic regime strongly influenced by the periodic dislocation of the ITCZ. This results from changes in the Atlantic meridional overturning circulation (Chiang and Bitz 2005) and/or tropical air–sea interactions, such as the El Niño and La Niña events (Broecker 2003). Therefore, one possibility is that, while a dry climate was in effect in other Amazonian areas, this site may have remained wet at least since the mid-Holocene under influence of the ITCZ dislocation dynamics.

On the other hand, considering the hypothesis of a dry Amazonia during the early and mid-Holocene, then a further hypothesis to be considered is that stabilization of the sea-level about 6000–5000 cal yr BP (Cohen et al. 2005b) may have attenuated the climate change, causing no impact on the vegetation cover. Existing RSL curves present dissimilar patterns for the late Holocene in Brazil. The first suggests a RSL fall in the last 5100 yr BP (5647–5999 cal yr BP) with two oscillations (Suguio et al. 1985a). Angulo and Lessa (1997) and Angulo et al. (1999) disagree with the low RSL between 4100–3800 yr BP (~4560– ~4130 cal yr BP) and 3000–2700 yr BP (~3100– ~2800 cal yr BP). Tomazelli (1990) suggests a RSL rise in the last 1000 years in the State of Rio Grande do Sul State.

Regarding the northern Brazilian littoral, the RSL stabilized at its current level between ~7000 and ~5000 cal yr BP (e.g., Behling and Costa 2001; Behling et al. 2001; Behling 2002, 2011; Cohen et al. 2005b; Souza Filho et al. 2006; Vedel et al. 2006). The history of RSL fluctuations on northern Brazilian littoral seems to have been affected by tectonic activity during the late Pleistocene and Holocene (Rossetti et al. 2008, 2012). The post-glacial sea-level rise, combined with tectonic subsidence, caused a marine transgression during the late Pleistocene and early Holocene along the northern Brazilian coast (Cohen et al. 2012). Between ~5100 and ~1000 cal yr BP, the RSL at the northern Brazil was probably never higher than 0.6 m above the current level (Cohen et al. 2005b). A work from the Lago do Crispim in the northeastern State of Pará, which is located next to the present coastline and only 1 m above msl, suggested no flooding during the last ~8800 cal yr BP (Behling and Costa 2001).

At the global scale, sea-level is the dominant driver of the water table depth (Fan et al. 2013). Then, sea-level changes during the Holocene might have influenced the shallow groundwater effects on terrestrial ecosystems by sustaining river base-flow and root-zone soil water in the absence of rain (Fan et al. 2013). Consequently, regarding a stable relative sea-level along the northern Brazilian littoral during the last 6000 cal yr BP (e.g., Behling et al. 2001; Cohen et al. 2005b, 2012; Vedel et al. 2006), the water table depth may have favored the establishment and maintenance of the Amazon lowland forest during the middle and late Holocene. Such event may have created an ecological barrier between a narrow aquatic zone, favoring the development of Amazonian lowland forests at the feet of a large belt of topographic higher hinterlands.

Eustatic sea-level changes since the Pleistocene have caused significant impact on the extent and composition of the Amazonian floodplain. As a consequence of the increased gradient, caused

https://doi.org/10.1017/RDC.2017.62 Published online by Cambridge University Press

by the decline of ca. 120 m in sea level during the LGM, the rivers cut deeply into their beds and a large volume of sediments were deposited in the Amazon fan (Junk 1997). At this time, river valleys became incised, and may have filled with fluvial deposits. Alternatively, the valleys may have remained essentially empty until the next transgression (Walker 1992). Geomorphological, sedimentological, and hydrological studies conducted along the Amazonian region upstream and downstream of the Negro River indicate that the *várzea* (floodplain) reached its present extent after sea-level stabilization, at 5000–6000 cal yr BP (Irion et al. 1997; Behling et al. 2002). Similar conclusion emerged from detailed examination of riverbed morphologies at the Amazon mouth (Junk 1994; Irion et al. 1997; Vital et al. 1998).

Regarding the present work, in order to obtain a pollen record since the early Holocene, some cores were sampled with depths up to 10 m. However, all ^{14}C dates obtained to the studied deposits indicated mid- and late Holocene. Although this study has not presented a pollen record since the early Holocene, the sediment deposits accumulated since ~4800 cal yr BP, from the base of the core RBN–83, may be an evidence for the time of the flood plain stabilization in a new level along the Branco River. Considering this hypothesis, the sea level rise during the early Holocene and its stabilization at the current level in the northern Brazilian coast, between 6000 and 5000 cal yr BP, may have caused the establishment of a fluvial terrace for accumulation of that sediments since the middle Holocene. Then, the absence of early Holocene sediments in the studied fluvial terrace may be related to the stabilization of the relative sea level in its modern level just in the middle Holocene. Older sedimentary deposits may have been eroded during the relative sea-level rise. Similar process was recorded for the Cardoso Island, São Paulo (Pessenda et al. 2012).

Today, the Amazon River and its tributaries are affected by dynamic tides, but without salt-water intrusion due to the high freshwater discharge, as far as 1100 km upstream of its mouth (Kosuth et al. 2009; Freitas et al. 2014). On the coastal zone, the stabilization of sea-level allowed development of wetlands (Cohen et al. 2012), while the rainfall inland favored expansion of forest vegetation, the development of perennial streams, and the diversification of terrestrial and aquatic fauna (Meggers 2007).

Therefore, if a dry climate occurred in Amazonia during the Holocene, the most likely is that the stabilization of the relative sea-level since the middle Holocene, may have contributed to the development of the Amazonian lowland forest, having attenuated the impact of the middle Holocene dry period on vegetation in areas under most fluvial influence. In this case, no major vegetation changes are expected after the stabilization of relative sea-level in areas affected by the Amazon drainage system. Studies carried out in the Amazon have shown a buffer effect for areas close to rainforest, where the forest reveals mechanisms of protection against drier periods (Pessenda et al. 1996).

CONCLUSIONS

Palynological analyses of fluvial deposits from the Branco River indicate a mixture of forest vegetation and herbaceous communities comparable to the modern one since the mid-Holocene. Then, significant vegetation changes did not occur in the study site during this time interval. The pollen data suggest a wet period similar to the modern one at least over the last 4808–4886 cal yr BP rather than a dry event in the mid-Holocene, as reported for many other Amazonian areas. One possibility is that Amazonia was never under the effect of a dry climate during most of the Holocene. Another hypothesis is that the impact of the dry period occurred during this time did not influence the studied site. On the other hand, taking into account a dry mid-Holocene climate, the stabilization of the relative sea-level, about 6000–5000 cal yr BP along the northern Brazilian

https://doi.org/10.1017/RDC.2017.62 Published online by Cambridge University Press

littoral, may have affected the water base level along the rivers, and it favored the establishment and maintenance of Amazonian lowland forests even under dry periods. Sea level may have attenuated the impact of dry periods in areas under fluvial influence.

ACKNOWLEDGMENTS

The authors wish to thank the Research Funding Institute of the State of São Paulo (FAPESP–Project #13/50475-5) for the financial support of this research. Brazil's National Council for Scientific and Technological Development provided research fellowships to the authors. The ICM-Bio-Chico Mendes Institute for Biodiversity Conservation helped with the logistic during the fieldwork.

REFERENCES

Ab'Saber A. 1989. Zoneamento ecológico e econômico da Amazônia: questões de escala e método. *Estud. Avançados* 3:4–20.

Absy ML. 1975. Polen e esporos do Quaternário de Santos (Brasil). *Hoehnea* 5:1–26.

Absy ML. 1979. A palynological study of Holocene sediments in the Amazon basin [PhD thesis]. University of Amsterdam. 86 p.

Absy ML, Cleef A, Fournier M, Martin L, Servant M, Sifeddine A, Silva MF, Soubiès F, Suguio K, Turcq B, Van der Hammen T. 1991. Mise en évidence de quatre phases d'ouverture de la forêt dense dans le sudest de l'Amazonie au cours des 60,000 dernières années. Première comparaison avec d'autres régions tropicales. *Compte Rendu de l'Académie des Sciences de Paris* 312:673–8.

Anderson AB. 1981. White-sand vegetation of Brazilian Amazonia. *Biotropica* 13:199–210.

Angulo RJ, Lessa GC. 1997. The Brazilian sea-level curves: a critical review with emphasis on the curves from the Paranaguá and Cananéia regions. *Marine Geology* 140:141–66.

Angulo RJ, Giannini PCF, Suguio K, Pessenda LCR. 1999. Relative sea-level changes in the last 5500 years in southern Brazil (Laguna-Imbituba region Santa Catarina State) based on vermitid ^{14}C ages. *Marine Geology* 159:323–39.

Behling H. 2002. Impact of the Holocene sea-level changes in coastal eastern and central Amazonia. *Amazoniana* 17:41–52.

Behling H. 2011. Holocene environmental dynamics in coastal eastern and central Amazonia and the role of the Atlantic sea-level change. *Geographica Helvetica* 3:208–16.

Behling H, Hooghiemstra H. 1998. Late Quaternary palaeoecology and palaeoclimatology from pollen records of the savannas of the Llanos Orientales in Colombia. *Palaeogeography Palaeoclimatology Palaeoecology* 139:251–67.

Behling H, Hooghiemstra H. 1999. Environmental history of the Colombian savannas of the Llanos Orientales since the Last Glacial Maximum from lake records El Pinal and Carimagua. *Journal of Paleolimnology* 21:461–76.

Behling H, Costa ML. 2000. Holocene environmental changes from the Rio Curuá record in the Caxiuanã region eastern Amazon Basin. *Quaternary Research* 53:369–77.

Behling H, Costa ML. 2001. Holocene vegetation and coastal environmental changes from Lago Crispim in northeastern Pará State northern Brazil. *Palaeogeography Palaeoclimatology Palaeoecology* 114: 145–55.

Behling H, Hooghiemstra H. 2000. Holocene Amazon rainforest–savanna dynamics and climatic implications: high-resolution pollen record from Laguna Loma Linda in eastern Colombia. *Journal of Quaternary Science* 15:687–95.

Behling H, Cohen MCL, Lara RJ. 2001. Studies on Holocene mangrove ecosystem dynamics of the Bragança Peninsula in northeastern Pará Brazil. *Palaeogeography Palaeoclimatology Palaeoecology* 167:225–42.

Behling H, Arz HW, Pätzold J, Wefer G. 2002. Late Quaternary vegetational and climate dynamics in southeastern Brazil inferences from marine cores GeoB 3229-2 and GeoB 3202-1. *Palaeogeography Palaeoclimatology Palaeoecology* 179:227–43.

Behling H, Cohen MCL, Lara RJ. 2004. Late Holocene mangrove dynamics of the Marajó Island in northern Brazil. *Vegetation History and Archaeobotany* 13:73–80.

Berrio JC, Hooghiemstra H, Behling H, Van der Borg K. 2000. Late Holocene history of savanna gallery forest from Carimagua area Colombia. *Review of Palaeobotany and Palynology* 111:295–308.

Bos JAA, Dambeck R, Kalis AJ, Schweizer A, Thiemeyer H. 2008. Palaeoenvironmental changes and vegetation history of the northern Upper Rhine Graben (southwestern Germany) Since the Lateglacial. *Netherlands Journal of Geosciences* 87:67–90.

Broecker WS. 2003. Does the trigger for abrupt climate change reside in the ocean or in the atmosphere? *Science* 300:1519–22.

Bush MB, Colinvaux PA. 1988. A 7000-year pollen record from the Amazon lowlands Ecuador. *Vegetation* 76:141–54.

https://doi.org/10.1017/RDC.2017.62 Published online by Cambridge University Press

Bush MB, Miller MC, de Oliveira PE, Colinvaux PA. 2000. Two histories of environmental change and human disturbance in eastern lowland Amazonia. *The Holocene* 10:543–53.

Bush MB, Silman MR, Listopad CMCS. 2007. A regional study of Holocene climate change and human occupation in Peruvian Amazonia. *Journal of Biogeography* 34:1342–56.

Castro DF, Rossetti DF, Pessenda LCR. 2010. Facies $\delta^{13}C$, $\delta^{15}N$, and C/N analyses in a late Quaternary compound estuarine fill northern Brazil and relation to sea level. *Marine Geology* 274:135–50.

Castro DF, Oliveira PE, Rossetti DF, Pessenda LCR. 2013. Late Quaternary landscape evolution of northeastern Amazonia from pollen and diatom record. *Anais da Academia Brasileira de Ciências* 85:35–55.

Chiang JCH, Bitz CM. 2005. Influence of high latitude ice cover on the marine Intertropical Convergence Zone. *Climate Dynamics* 25:477–96.

Cohen MCL, Behling H, Lara RJ. 2005a. Amazonian mangrove dynamics during the last millennium: the relative sea-level and the little Ice Age. *Review of Palaeobotany and Palynology* 136: 93–108.

Cohen MCL, Souza Filho PW, Lara RL, Behling H, Angulo R. 2005b. A model of Holocene mangrove development and relative sea-level changes on the Bragança. Peninsula (northern Brazil). *Wetlands Ecology and Management* 13:433–43.

Cohen MCL, Lara RJ, Smith CB, Angélica RS, Dias BS, Pequeno T. 2008. Wetland dynamics of Marajó Island northern Brazil during the last 1000 years. *Catena* 76:70–7.

Cohen MCL, Lara RJ, Smith CB, Matos HRS, Vedel V. 2009. Impact of sea level and climatic changes on the Amazon coastal wetlands during the late Holocene. *Vegetation History and Archaeobotany* 18:425–39.

Cohen MCL, Pessenda LCR, Behling H, Rossetti DF, França MC, Guimarães JTF, Friaes YS, Smith CB. 2012. Holocene palaeoenvironmental history of the Amazonian mangrove belt. *Quaternary Science Reviews* 55:50–8.

Cohen MCL, Rossetti DF, Pessenda LCR, Friaes YS, Oliveira PE. 2014. Late Pleistocene glacial forest of Humaitá—Western Amazonia. *Palaeogeography Palaeoclimatology Palaeoecology* 415c:48–58.

Colinvaux PA, De Oliveira PE, Moreno JE, Miller MC, Bush MB. 1996. A long pollen record from lowland Amazonia: forest and cooling in glacial times. *Science* 247:85–8.

Colinvaux P, De Oliveira PE, Patiño JEM. 1999. *Amazon Pollen Manual and Atlas*. Dordrecht: Harwood Academic Publishers. 332 p.

Cordeiro RC, Turcq PFM, Turcq BJ, Moreira LS, Rodrigues RC, Costa RL, Sifeddine A, Simões Filho FFL. 2008. Acumulação de carbono em lagos amazônicos como indicador de eventos paleoclimaticos e antrópicos. *Oecol. Bras* 12: 130–54.

Cordeiro RC, Turcq BJ, Sifeddine A, Lacerda LD, Silva Filho EV, Gueiros BB, Cunha YPP, Santelli RE, Pádua EO, Pachinelam SR. 2011. Biogeochemical indicators of enviromnental changes from 50 ka to 10 ka. *Palaeogeography Palaeoclimatology Palaeoecology* 299:426–36.

Davis MB. 2000. Palynology after Y2K—understanding the source area of pollen in sediments. *Annual Review of Earth and Planetary Science* 28:1–18.

Desjardins T, Filho AC, Mariotti A, Chauvel A, Girardin C. 1996. Changes of the forest savanna boundary in Brazilian Amazonia during the Holocene as revealed by soil organic carbon isotope ratios. *Oecologia* 108:749–56.

Faegri K, Iversen J. 1989. *Textbook of Pollen Analysis*, 4th Ed. New York: John Wiley & Sons.

Fan Y, Li H, Miguez-Macho G. 2013. Global patterns of groundwater table depth. *Science* 339:940–3.

França MC, Francisquini MI, Cohen MCL, Pessenda LCR, Rossetti DF, Guimarães JTF, Smith CB. 2012. The last mangroves of Marajó Island—Eastern Amazon: impact of climate and/or relative sea-level changes. *Review of Paleobotany and Palynology* 187:50–65.

Freitas HA, Pessenda LCR, Aravena R, Gouveia SEM, Ribeiro AS, Boulet R. 2001. Late Quaternary vegetation dynamics in the southern Amazon basin inferred from carbon isotopes in soil organic matter. *Quaternary Research* 55:39–46.

Freitas PTA, Silva MS, Souza Filho PWM, Ogston A, Nittrouer CA, Asp NE. 2014. Tidal influence on the hydrodynamics in a major Amazon tributary. *Proceedings of the 17th Physics of Estuaries and Coastal Seas (PECS) Conference*. Porto de Galinhas Pernambuco, Brazil.

Gosling WD, Mayle FE, Tate NJ, Killeen TJ. 2009. Differentiation between neotropical rainforest dry forest and savanna ecosystems by their modern pollen spectra and implications for the fossil pollen record. *Reviews of Palaeobotany and Palynology* 153:70–85.

Gouveia SEM, Pessenda LCR, Aravena R, Boulet R, Roveratti R, Gomes BM. 1997. Dinâmica de vegetações durante o Quaternário recente no sul no Amazonas indicada pelos isótopos do carbono (^{12}C ^{13}C ^{14}C) do solo. *Geochimica Brasiliensis* 11:335–67.

Gribel R, Ferreira CAC, Coelho LS, Santos JL, Ramos J F, Silva KAF. 2009. Vegetação do Parque Nacional do Viruá–RR. Relatório Técnico. Brasília: Instituto Chico Mendes de Conservação da Biodiversidade (ICMBio).

Grimm EC. 1987. CONISS: a Fortran 77 program for stratigraphically constrained cluster analysis by the method of the incremental sum of squares. *Pergamon Journal* 13:13–35.

Guimarães JTF, Cohen MCL, França MC, Lara RJ, Behling H. 2010. Model of wetland development of the Amapá littoral during the Late Holocene. *Anais da Academia Brasileira de Ciências* 82:1–15.

https://doi.org/10.1017/RDC.2017.62 Published online by Cambridge University Press

Hermanowski B, Costa ML, Carvalho AT, Behling H. 2012. Palaeoenvironmental dynamics and underlying climatic changes in southeast Amazonia (Serra Sul dos Carajás Brazil) during the late Pleistocene and Holocene. *Palaeogeography Palaeoclimatology Palaeoecology* 365–366: 227–46.

Howard AJ, Gearey B, R Hill T, Fletcher W, Marshall P. 2009. Fluvial sediments correlations and palaeoenvironmental reconstruction: the development of robust radiocarbon chronologies. *Journal of Archaeol. Science* 36:2680–8.

Instituto Brasileiro de Geografia e Estatística – IBGE. 2012. *Manuais Técnicos em Geociências – número 1*, Manual Técnico da Vegetação Brasileira– Sistema fitogeográfico Inventário das formações florestais e campestres Técnicas e manejo de coleções botânicas Procedimentos para mapeamentos. Rio de Janeiro: IBGE/ Ministério do Planejamento Orçamento e Gestão. 271 p.

Irion G, Bush MB, Nunes de Mello JA, Stüben D, Neumann T, Müller G, Morais de JO, Junk JW. 2006. A multiproxy palaeoecological record of Holocene lake sediments from the Rio Tapajós eastern Amazonia. *Palaeogeography Palaeoclimatology Palaeoecology* 240:523–35.

Irion G, Junk WJ, Mello JASN de. 1997. The large Central Amazonian River floodplains near Manaus: geological climatological hydrological and geomorphological aspects. In: Junk WJ, editor. *The Central Amazon Floodplain*. Berlin: Springer Verlag. p 23–46.

Jacob J, Huang Y, Disnar JR, et al. 2007. Paleohydrological changes during the last deglaciation in Northern Brazil. *Quaternary Science Reviews* 26:1004–15.

Junk WJ. 1994. Ecology of the várzea floodplain of Amazonian whitewater rivers. In: Harald Sioli, editor. *The Amazon-Limnology and Landscape Ecology of a Mighty Tropical River and Its Basin*. Netherlands: Springer. p 215–43.

Junk WJ, editor. 1997. *The Central Amazon Floodplain Ecological Studies*. Berlin: Springer.

Kasse C, Hoek WZ, Bohncke SJP, Konert M, Weijers JWH, Cassee ML, Van der Zee RM. 2005. Late Glacial fluvial response of the Niers-Rhine (western Germany) to climate and vegetation change. *Journal of Quaternary Science* 20:377–94.

Kosuth P, Calléde J, Laraque A, Filizola N, Guyot JL, Seyler P, Fritsch JM, Guimarães V. 2009. Sea-tide effects on flows in the lower reaches of the Amazon River. *Hydrological Processes* 23:3141–50.

Laranjeiras TO, Naka LN, Bechtoldt CL, da Costa TVV, Andretti CB, Cerqueira MC, de Fátima Torres M, Rodrigues GL, Santos MPD, Vargas CF, Pacheco AMF, Sardelli CH, Mazar-Barnett J, Cohn-Haft M. 2014. The avifauna of Viruá National Park Roraima reveals megadiversity in northern Amazonia. *Revista Brasileira de Ornitologia* 22:138–71.

Latrubesse EM. 2002. Evidence of Quaternary palaeohydrological changes in middle Amazônia: the Aripuanã-Roosevelt and Jiparaná fans. *Z. Geomorphol* 129:61–72.

Latrubesse EM, Ramonell CG. 1994. A climatic model for southwestern Amazonia in last glacial times. *Quaternary International* 21:163–9.

Latrubesse EM, Nelson BW. 2001. Evidence for Late Quaternary aeolian activity in the Roraima-Guyana Region. *Catena* 43:63–80.

Ledru MP, Ceccantini G, Gouveia SEM, Lopez–Sáez JA, Pessenda LCR, Ribeiro AS. 2006. Millenial-scale climatic and vegetation changes in a northern Cerrado (northeast Brazil) since the Last Glacial Maximum. *Quaternary Science Reviews* 25:1110–26.

Lowe JJ, Walker MJC, Scott EM, Harkness DD, Bryant CL, Davies SM. 2004. A coherent high-precision radiocarbon chronology for the Late-glacial sequence at Sluggan Bog Co. Antrim Northern Ireland. *Journal of Quaternary Science* 19:147–58.

Macario K, Gomes PRS, Anjos RM, Carvalho C, Linares R, Alves EQ, Oliveira FM, Castro MD, Chanca IS, Silveira MFM, Pessenda LCR, Moraes LMB, Campos TB, Cherkinsky A. 2013. The Brazilian AMS Radiocarbon Laboratory (LAC–UFF) and the intercomparison of results with CENA and UGAMS. *Radiocarbon* 55(2): 325–30.

Markgraf V, D'Antoni HL. 1978. *Pollen Flora of Argentina*. Tucson: University of Arizona Press.

Maslin MA, Burns SJ. 2000. Reconstruction of the Amazon Basin effective moisture availability over the past 14,000 years. *Science* 290:2285–7.

Mayle FE, Burbridge R, Killeen TJ. 2000. Millennial-scale dynamics of southern Amazonian rain forests. *Science* 290:2291–4.

Mayle FE, Power MJ. 2008. Impact of a drier Early-Mid-Holocene climate upon Amazonian forests. *Phil. Trans. R. Soc. B* 363:1829–38.

Meggers BJ. 2007. Mid-Holocene climate and cultural dynamics in Brazil and the Guianas. In: Anderson DG, Maasch KA, Sandweiss DH, editors. *Climate Change and Cultural Dynamics: A Global Perspective on Mid-Holocene Transitions*, p 117–55.

Miranda ACC, Rossetti DF, Pessenda LCR. 2009. Quaternary paleoenvironments and relative sea–level changes in Marajó Island (Northern Brazil): facies, $\delta^{13}C$ $\delta^{15}N$ and C/N. *Palaeogeography Palaeoclimatology Palaeoecology* 282:19–31.

Moreira LS, Moreira-Turcq P, Turcq B, Caquineau S, Cordeiro RC. 2012. Paleohydrological changes in an Amazonian floodplain lake: Santa Ninha Lake. *Journal of Paleolimnology* 48:339–50.

Mosblech NAS, Bush MB, Gosling WD, Hodell D, Thomas L, Van Calsteren P, Correa-Metrio A, Valencia BG, Curtis J, Van Woesik R. 2012. North Atlantic forcing of Amazonian precipitation during the Last Ice Age. *Nat. Geosci* 5:817–20.

https://doi.org/10.1017/RDC.2017.62 Published online by Cambridge University Press

Pessenda LCR, Valencia EPE, Martinelli LA, Cerri CC. 1996. ^{14}C measurements in tropical soil developed on basic rocks. *Radiocarbon* 38(2):203–8.

Pessenda LCR, Gomes BM, Aravena R, Ribeiro AS, Boulet R, Gouveia SEM. 1998a. The carbon isotope record in soils along a forest-cerrado ecosystem transect: implications for vegetation changes in the Rondonia state southwestern Brazilian Amazon region. *The Holocene* 8.5: 599–603.

Pessenda LCR, Gouveia SEM, Aravena R, Gomes BM, Boulet R, Ribeiro AS. 1998b. ^{14}C dating and stable carbon isotopes of soil organic matter in forest savanna boundary areas in the southern Brazilian Amazon region. *Radiocarbon* 40:1013–22.

Pessenda LCR, Gouveia SEM, Gomes BM, Boulet R, Ribeiro AS. 1998c. Studies of paleovegetation changes in the central Amazon by carbon isotopes (^{12}C ^{13}C ^{14}C) of soil organic matter. Isotope techniques in the study of environmental change. Proceedings of a symposium, Vienna, April 1997. p 645–52.

Pessenda LCR, Boulet R, Aravena R, Rosolen V, Gouveia SEM, Ribeiro AS, Lamotte M. 2001. Origin and dynamics of soil organic matter and vegetation changes during the Holocene in a forest–savanna transition zone Brazilian Amazon region. *The Holocene* 11:250–4.

Pessenda LCR, Ribeiro AS, Gouveia SEM, Aravena R, Boulet R, Bendassoli JA. 2004. Vegetation dynamics during the late Pleistocene in the Barreirinhas region Maranhão State northeastern Brazil based on carbon isotopes in soil organic matter. *Quaternary Research* 62:183–93.

Pessenda LCR, Vidotto E, De Oliveira PE, Buso AA, Cohen MCL, Rossetti D, de Ricardi-Branco F, Bendassolli JA. 2012. Late Quaternary vegetation and coastal environmental changes at Ilha do Cardoso mangrove southeastern Brazil. *Palaeogeography Palaeoclimatology Palaeoecology* 363:57–68.

RADAMBRASIL. 1975. Departamento Nacional de Produção Mineral. Projeto Radam. Folha NA–20 Boa Vista e parte das folhas NA-21 Tumucumaque NB-20 Roraima e NB–21: geologia geomorfologia pedologia vegetação e uso potencial da terra. *Rio de Janeiro: DNPM* 1975. 428 p.

RADAMBRASIL Project. 1976. *Folha NA-20 Boa Vista: geologia geomorfologia pedologia vegetação e uso potencial da terra*. Departamento Nacional de Produção Mineral: Rio de Janeiro.

Räsänen M, Salo J, Kalliola R. 1987. Fluvial perturbance in the western Amazon basin: regulation by long term sub-Andean tectonics. *Science* 238:1398–401.

Reimer P. 2013. IntCal13 and Marine13 radiocarbon age calibration curves 0–50,000 years cal BP. *Radiocarbon* 55:1869–87.

Rigsby CA, Hemric EM, Baker PA. 2009. Late Quaternary paleohydrology of the Madre de Dios River southwestern Amazon Basin, Peru. *Geomorphology* 113:158–72.

Rossetti DF, Toledo PM, Moraes-Santos HM, Santos Jr AEA. 2004. Reconstructing habitats in central Amazonia using megafauna sedimentology radiocarbon and isotope analyses. *Quaternary Research* 61:289–300.

Rossetti DF, Toledo PM, Góes AM. 2005. New geological framework for Western Amazonia (Brazil) and implications for biogeography and evolution. *Quaternary Research* 63:78–89.

Rossetti DF, Valeriano MM, Goes AM, Thales M. 2008. Palaeodrainage on Marajó Island northern Brazil in relation to Holocene relative sea-level dynamics. *The Holocene* 18:01–12.

Rossetti DF, Souza LSB, Prado R, Elis VR. 2012. Neotectonics in the northern equatorial Brazilian margin. *Journal of South American Earth Sciences* 37:175–90.

Rossetti DF, Zani H, Cremon EH. 2014. Fossil megafans evidenced by remote sensing in the Amazonian wetlands. *Zeitschrift fur Geomorphologie* 58:145–61.

Rossetti DF, Polizel SP, Cohen MCL, Pessenda LCR. 2015. Late Pleistocene–Holocene evolution of the Doce River delta southeastern Brazil: implications for the understanding of wave-influenced deltas. *Mar. Geol* 367:171–90.

Roubik DW, Moreno JE. 1991. *Pollen and Spores of Barro Colorado Island*. St. Louis, MO: Missouri Botanical Garden. 268 p.

Ruter A, Arzt J, Vavrus S, et al. 2004. Climate and environment of the subtropical and tropical Americas (NH) in the mid-Holocene: comparison of observations. *Quaternary Science Reviews* 23:663–79.

Salgado-Labouriau M.L. 1973. *Contribuição à palinologia dos cerrados*. Rio de Janeiro: Academia Brasileira de Ciências. 273 p.

Santos JOS, Nelson BW, Geovannini CA. 1993. Os campos de dunas do Pantanal Setentrional. *Ciência Hoje* 16(93):22–5.

Serruya NM. 2002. Zoneamento Ecológico Econômico da Região Central do Estado de Roraima tomo II. Volume II: Diagnóstico do Meio Bióticо-Cobertura Vegetal e Áreas Alteradas. *CPRM–Serviço Geológico do Brasil* p. 90–101.

Shackleton NJ. 1988. Oxygen isotopes ice volume and sea level. *Quaternary Science Reviews* 6: 183–90.

Sifeddine A, Bertrand P, Fournier M, Martin L, Servant M, Soubiès F, Suguio K, Turcq B. 1994. La sédimentation organique lacustre en milieu tropical humide (Carajás Amazonie orientale Brésil): relation avec les changements climatiques au cours des 60000 dernières années. *Bulletin de La Société Geologique de France* 165:613–21.

Sifeddine A, Marint L, Turcq B, Volkmer-Ribeiro C, Soubiès F, Cordeiro RC, Suguio K. 2001. Variations of the Amazonian rainforest environment: a sedimentological record covering 30,000 years. *Palaeogeography Palaeoclimatology Palaeoecology* 168:221–35.

https://doi.org/10.1017/RDC.2017.62 Published online by Cambridge University Press

Souza Filho PWM, Martins ESF, Costa FR. 2006. Using mangroves as a geological indicator of coastal changes in the Bragança macrotidal flat Brazilian Amazon: a remote sensing data approach. *Ocean and Coastal Management* 49:462–75.

Stuiver M, Polach HA. 1977. Discussion: reporting of ^{14}C data. *Radiocarbon* 19:355–63.

Suguio K, Martin L, Bittencourt ACSP, Dominguez JML, Flexor JM, Azevedo AEG. 1985a. Flutuações do Nível do Mar durante o Quaternário Superior ao longo do Litoral Brasileiro e suas Implicações na Sedimentação Costeira. *Revista Brasileira de Geociência* 15:273–86.

ter Steege H, Jetten VG, Polak AM, et al. 1993. Tropical rain forest types and soil factors in a watershed area in Guyana. *Journal of Vegetation Science* 4:705–16.

Tomazelli LJ. 1990. Contribuição ao estudo dos sistemas deposicionais Holocênicos do Nordeste da Província Costeira do Rio Grande do Sul com Ênfase no Sistema Eólico [PhD thesis]. Porto Alegre Universidade Federal do Rio Grande do Sul. 270 p.

Toonen WHJ, Kleinhans MG, Cohen KM. 2012. Sedimentary architecture of abandoned channel fills. *Earth Surf. Process. Landforms* 37:459–72.

Turney CSM, Coope GR, Harkness DD, Lowe JJ, Walker MJC. 2000. Implications for the dating of Wisconsinan (Weichselian) Late-Glacial events of systematic radiocarbon age differences between terrestrial plant macrofossils from a site in SW Ireland. *Quaternary Research* 53:114–21.

Van der Hammen T, Duivenvoorden JF, Lips JM, Urrego LE, Espejo N. 1992. The late Quaternary of the middle Caquetá area (Colombian Amazonia). *Journal of Quaternary Sciences* 7:45–55.

Vedel V, Behling H, Cohen MCL, Lara RJ. 2006. Holocene mangrove dynamics and sea-level changes in Taperebal northeastern Pará State northern Brazil. *Vegetation History and Archaeobotany* 15:115–23.

Veloso HP, Rangel-Filho ALR, Lima JCA. 1991. *Classificação da Vegetação Brasileira Adaptada a um Sistema Universal*. Rio de Janeiro: Instituto Brasileiro de Geografia e Estatística.

Vital H, Stattegger K, Posewang J, Theilen F. 1998. Lowermost Amazon River: morphology and shallow seismic characteristics. *Mar. Geol* 152:277–94.

Vormisto J, Phillips OL, Ruokolainen K, et al. 2000. A comparison of fine-scale distribution patterns of four plant groups in an Amazonian rainforest. *Ecography* 23:349–59.

Walker RG. 1992. Facies facies models and modern stratigraphic concepts. In: Walker RG, James NP, editors. *Facies Models—Response to Sea Level Change*. Ontario: Geological Association of Canada. p 1–14.

Weng C, Bush MB, Athens JS. 2002. Two histories of climate change and hydrarch succession in Ecuadorian Amazonia. *Review of Paleobotany and Palynology* 120:73–90.

Weng C, Bush MB, Silman MR. 2004b. An analysis of modern pollen rain on na elevational gradient in southern Peru. *Journal Trop. Ecology* 20:113–24.

Wentworth CK. 1922. A scale of grade and class terms for clastic sediments. *J. Geol.* 30:377–92.

Xu Q, Tian F, Bunting MJ, Li Y, Ding W, Cao X, He Z. 2012. Pollen source areas of lakes with inflowing rivers: modern pollen influx data from Lake Baiyangdian China. *Quaternary Science Review* 37:81–91.

Zani H, Rossetti DF, Cohen MLC, Pessenda LCR, Cremon EH. 2012. Influence of landscape evolution on the distribution of floristic patterns in northern Amazonia revealed by $\delta^{13}C$ data. *Journal of Quaternary Science* 27:854–64.

https://doi.org/10.1017/RDC.2017.62 Published online by Cambridge University Press